IL NUOVO CIMENTO Vol. 36 C, N. 6 Novembre-Dicembre 2013
DOI 10.1393/ncc/i2014-11611-0

Colloquia: LaThuile13

Search for neutrinoless double beta decay with the GERDA experiment

C. Macolino for the GERDA Collaboration
INFN, Laboratori Nazionali del Gran Sasso (LNGS) - Assergi (AQ), Italy

ricevuto il 20 Giugno 2013; approvato l'1 Luglio 2013

Summary. — The GERmanium Detector Array, GERDA, is designed to search for neutrinoless double beta ($0\nu\beta\beta$) decay of ^{76}Ge and it is installed in the Hall A of the Laboratori Nazionali del Gran Sasso (LNGS) of INFN, Italy. The new shielding concept of GERDA is implemented by operating bare Ge (enriched in ^{76}Ge) detectors in cryogenic liquid argon, surrounded by an additional shield of ultra-pure water. The aim of GERDA is to verify the recent claim of discovery based on data of the Heidelberg-Moscow experiment and, in a second phase, to reach a background level two orders of magnitude lower than previous experiments. In this paper the GERDA experimental setup and future updates are described. Also, the results about the measurement of the two neutrino double beta decay half-life of ^{76}Ge are reported and discussed.

PACS 14.60.Pq – Neutrino mass and mixing.
PACS 23.40.-s – β decay; double β decay; electron and muon capture.

1. – Introduction

Recent results about neutrino flavour oscillations showed the evidence of non-zero neutrino mass and provided the values for Δm^2, the differences of the squared masses of the neutrino mass eigenstates. Nevertheless many neutrino properties have still to be measured. Neutrinoless double beta ($0\nu\beta\beta$) decay can give additional information about the absolute neutrino mass scale and also on the possibility for the neutrino to have a Majorana nature, *i.e.* if it coincides with its own antiparticle.

Neutrinoless double beta decay is a lepton number violating process that can be viewed as the ordinary two neutrino double beta decay ($2\nu\beta\beta$),

$$(A, Z) \rightarrow (A, Z + 2) + 2e^- + 2\bar{\nu}_e, \tag{1}$$

where the two antineutrinos annihilate. The GERDA experiment [1,2] searches for neutrinoless double beta decay of ^{76}Ge, in which the ^{76}Ge ($Z = 32$) would decay into ^{76}Se ($Z = 34$) and two electrons. The $0\nu\beta\beta$ decay can be experimentally observed as a narrow peak at the $Q_{\beta\beta}$-value of the decay. While the two-neutrino double beta decay is not forbidden by any conservation law in the Standard Model, $0\nu\beta\beta$ can occur only if the

neutrino has a non-zero mass and is a Majorana particle. Theoretical models predict that $0\nu\beta\beta$ would be mediated by a light Majorana neutrino. In such a case the half-life of the decay can give direct information on the effective Majorana neutrino mass:

$$\frac{1}{T^{0\nu}_{1/2}(A,Z)} = F^{0\nu} \cdot |\mathcal{M}^{0\nu}|^2 \cdot |m_{\beta\beta}|^2, \tag{2}$$

where $F^{0\nu}$ is the phase space factor, $\mathcal{M}^{0\nu}$ is the nuclear matrix element (NME) and $m_{\beta\beta} = \sum U^2_{ei} m_i$ is the effective Majorana mass, with U_{ei} the elements of the neutrino mixing matrix and m_i the masses of the neutrino mass eigenstates.

The High-Purity-Germanium (HPGe) detectors, implemented in the GERDA setup, are semiconductors made from material with isotope fraction of ^{76}Ge enriched to about 86% (^{enr}Ge), which act as both the $\beta\beta$ decay source and a 4π detector. They are characterized by a very good energy resolution and allow a clear distinction of the neutrinoless double beta peak at $Q_{\beta\beta} = 2039\,\text{keV}$. The best limits for $0\nu\beta\beta$ decay in ^{76}Ge have been provided by the Heidelberg-Moscow (HdM) [3] and IGEX [4] enriched ^{76}Ge experiments, yielding lower half-life limits of about $T_{1/2} > 1.9 \cdot 10^{25}\,\text{yr}$ and $T_{1/2} > 1.6 \cdot 10^{25}\,\text{yr}$, respectively, corresponding to an upper limit on the effective Majorana mass of $|m_{\beta\beta}| < 0.33$–$1.35\,\text{eV}$, being the given range due to the estimated uncertainty in the nuclear matrix elements. A fraction of the HdM Collaboration claimed the observation of $0\nu\beta\beta$ with a half-life of $T^{0\nu}_{1/2} = 1.2^{+3.0}_{-0.5} \cdot 10^{25}\,\text{yr}$ (3σ range), corresponding to a value for $|m_{\beta\beta}|$ between 0.1 and 0.9 eV, with the central value of 0.44 eV [5]. In a more sophisticated analysis, the authors found a value for the half-life equal to $T^{0\nu}_{1/2} = 2.2^{+0.4}_{-0.3} \cdot 10^{25}\,\text{yr}$ [6]. The aim of the GERDA experiment is to verify such results and to reach a much higher sensitivity than previous experiments, with an ultimate sensitivity value for the half-life $T^{0\nu}_{1/2} > 1.4 \cdot 10^{26}\,\text{yr}$ at 90% confidence level, corresponding to a $|m_{\beta\beta}|$ range between 0.1 and 0.3 eV. In the current first phase of GERDA an exposure of about $15\,\text{kg} \cdot \text{yr}$ has been reached after one year of data taking. The target sensitivity will be reached in the GERDA second phase, when the total mass for the ^{76}Ge enriched detectors will exceed 20 kg and new methods for background suppression will be implemented.

2. – Experimental setup

The concept design of GERDA [7] is implemented by operating bare ^{enr}Ge detectors in the cryogenic liquid argon (LAr) [8]. Liquid argon, indeed, acts as both the coolant medium for the Ge detectors and the shield against external gamma radiation. In fig. 1 an artist's view of the GERDA experiment is shown (the Ge array is not to scale). The array of germanium detectors is suspended in strings into the cryostat which contains the liquid argon. The cryostat is a steel vessel of 4 m diameter with a copper lining, in order to reduce the gamma radiation from the steel vessel. Radon can also emanate from the vessel walls and be transported by convection close to the Ge diodes. To prevent this, the central volume of the cryostat (of about 3 m height and 750 mm diameter) is separated from the rest by a cylinder, made of a $30\,\mu$m thick copper foil, called the "radon shroud". The cryostat is placed in a large tank (8.5 m high and 10 m of diameter) filled with ultra-pure water, providing a 3 m thick water buffer around the cryostat. The water buffer purpose is: i) to moderate and absorb neutrons, ii) to attenuate the flux of external γ radiation, iii) to serve as Cherenkov medium for the detection of muons and iv) to provide a backup for the LNGS cooling water, which could be needed to heat

Fig. 1. – Artist's view of the GERDA experiment. The detector array is not to scale.

the argon gas in case of emergency. The fraction of ions normally existing in the water, as U, Th and K, are kept on the orders of fractions of ppm by the water plant, which also has the function to control the level of the Total Organic Carbon (TOC), otherwise the water would go in a gradual degradation of its optical transparency. A cleanroom and the lock, located on the top of the vessel, allow to insert and remove the detector strings without contaminating the cryogenic volume and also to enter calibration sources inside the cryostat. The water tank is instrumented with 66 PMTs facing inwards into the cryostat. They detect the Cherenkov light produced by muon induced showers. Additionally, an array of 36 plastic scintillators panels are installed on the roof of the clean room. Cherenkov and scintillation signals are combined according to a logic OR as a muon veto for the germanium DAQ.

In its first phase, GERDA uses 6 p-type ^{76}Ge coaxial (High Purity Germanium) detectors, from the previous HdM and IGEX experiments, with a total mass of about 14.6 kg, plus a natural Ge detector with a mass of 3 kg. In addition to these detectors, 5 Broad Energy GErmanium (BEGes) diodes (manufactured by Canberra, Olen Belgium), foreseen for the phase II of the experiment, have been also deployed, in order to test them in a realistic environment. The total working mass for the BEGes is about 3 kg. The detector array has a hexagonal structure and is made up of individual strings, each of them containing up to five independent Ge detector modules. The energy scale is determined by performing energy calibrations with sources of ^{228}Th on a weekly basis. The energy spectra of the six coaxial detectors are shown in fig. 2. The peaks are well fitted by a Gaussian function and an error function representing the background. The red lines represent the fit and the FWHM of the Gaussian is given in keV. From the fitted FWHM at 2614.5 keV, the extrapolated values for the resolutions at $Q_{\beta\beta} = 2039$ keV give a mass weighted average of 4.5 keV [7]. BEGe detectors have lower capacitance, which translates into better energy resolution. The mass weighted average at $Q_{\beta\beta} = 2039$ keV is about 3.0 keV.

3. – Background sources and background level in GERDA

The experimental setup of GERDA allows to reduce sensitively both external and internal backgrounds by the use of the multilevel passive shields and by reducing the amount of materials around the naked Ge detectors. The 3 m thick layer of highly

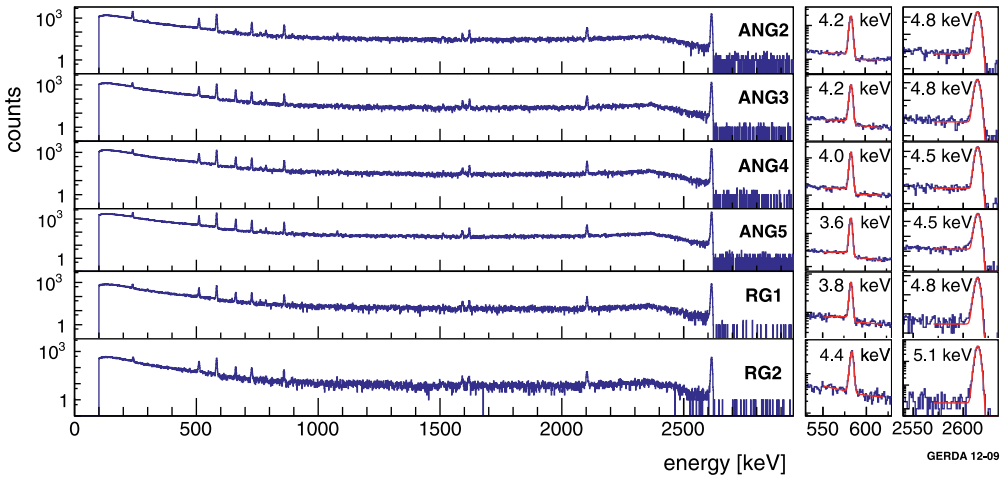

Fig. 2. – The energy spectra of the six enriched germanium detectors are plotted for a calibration with ^{228}Th. The fit results for the 583.2 keV and the 2614.5 keV lines including the values for a Gaussian FWHM are shown on the right.

purified water plus the 2 m thick cryogenic shield reduce the radioactivity of the rock and concrete (~ 3 Bq/kg ^{228}Th) to a background index of a few 10^{-4} counts/(keV·kg·yr) [9]. Also, additional contributions from the construction materials are minimized by using selected materials with extremely low radioactive contamination. Finally the active shield of Cherenkov detector and plastic scintillator array reduces the external background produced by cosmic rays to a level $< 10^{-4}$ counts/(keV·kg·yr) [10].

The internal background for the Ge detectors is mainly due to cosmogenic spallation in germanium, given by ^{60}Co and ^{68}Ge, since their lifetimes are of the order of years and their decay products can produce events in the region of interest. To minimize such background, the exposure of Ge diodes to cosmic rays is reduced as much as possible. Active methods of internal background reduction are also possible, taking into account that $\beta\beta$ decay has a point-like deposition of energy while the gammas from ^{60}Co and ^{68}Ge decays deposit their energy in more than one detectors, since they undergo into multiple Compton interactions. Indeed, these "multi-site" events are rejected by asking for anti-coincidence in the detectors. For the GERDA phase II it is foreseen to use the identification of multi-site events from the time structure of the signal (pulse-shape analysis) and to detect the scintillation light of LAr. Monte Carlo simulations demonstrate that, applying these two additional techniques, the background level will reach values less than 10^{-3} counts/(keV·kg·yr) [11].

In the very first phase of GERDA data taking a very high background was observed ($18 \cdot 10^{-2}$ counts/(keV·kg·yr). Also, the line at 1525 keV from ^{42}K, the progeny of ^{42}Ar, had an intensity in the energy spectrum much higher than expected [12]. These observations suggested the hypothesis that charged ions of ^{42}K drifted in the electric field produced by the 3 to 4 kV bias of the bare Ge diodes. For this reason, the strings of detectors were enclosed into 60 μm thick copper cylinders, called "mini-shrouds". The resulting background index shows a clear improvement compared to previous experiments. The intensity of gamma lines in the energy spectrum of GERDA has been investigated to identify the sources of background [7]. The results are shown in table I for both the natural and the enriched coaxial detectors, together with the values reported by the HdM

TABLE I. – *Counts and rates of background lines for the enriched and natural detectors in GERDA in comparison to the enriched detectors of HdM* [13].

		^{nat}Ge (3.17 kg·yr)		^{enr}Ge (6.10 kg·yr)		HDM (71.7 kg·yr)
Isotope	Energy	tot/bck	rate	tot/bck	rate	rate
	[keV]	[cts]	[cts/(kg·yr)]	[cts]	[cts/(kg·yr)]	[cts/(kg·yr)]
^{40}K	1460.8	85/15	$21.7^{+3.4}_{-3.0}$	125/42	$13.5^{+2.2}_{-2.1}$	181 ± 2
^{60}Co	1173.2	43/38	< 5.8	182/152	$4.8^{+2.8}_{-2.8}$	55 ± 1
	1332.3	31/33	< 3.8	93/101	< 3.1	51 ± 1
^{137}Cs	661.6	46/62	< 3.2	335/348	< 5.9	282 ± 2
^{228}Ac	910.8	54/38	$5.1^{+2.8}_{-2.9}$	294/303	< 5.8	29.8 ± 1.6
	968.9	64/42	$6.9^{+3.2}_{-3.2}$	247/230	$2.7^{+2.8}_{-2.5}$	17.6 ± 1.1
^{208}Tl	583.2	56/51	< 6.5	333/327	< 7.6	36 ± 3
	2614.5	9/2	$2.1^{+1.1}_{-1.1}$	10/0	$1.5^{+0.6}_{-0.5}$	16.5 ± 0.5
^{214}Pb	352	740/630	$34.1^{+12.4}_{-11.0}$	1770/1688	$12.5^{+9.5}_{-7.7}$	138.7 ± 4.8
^{214}Bi	609.3	99/51	$15.1^{+3.9}_{-3.9}$	351/311	$6.8^{+3.7}_{-4.1}$	105 ± 1
	1120.3	71/44	$8.4^{+3.5}_{-3.5}$	194/186	< 6.1	26.9 ± 1.2
	1764.5	23/5	$5.4^{+1.9}_{-1.5}$	24/1	$3.6^{+0.9}_{-0.8}$	30.7 ± 0.7
	2204.2	5/2	$0.8^{+0.8}_{-0.7}$	6/3	$0.4^{+0.4}_{-0.4}$	8.1 ± 0.5

Collaboration [13]. The energy spectra for the enriched and natural detectors are shown in fig. 3. The green boxes indicate the blinded window of 20 keV around the $Q_{\beta\beta}$ value. The low energy part of the spectrum is dominated by the β decay of ^{39}Ar which has an endpoint of 565 keV. Events from $2\nu\beta\beta$ decay in the range from 600 to 1400 keV are also cleary visible in the spectrum. At energies above 4000 keV a background contribution from α decay of ^{210}Po is dominant. The average BI, calculated in a $\pm$100 keV window around the $Q_{\beta\beta}$ value, is: (2.2 ± 0.3) counts/(keV·kg·yr) for the enriched coaxial detectors; $(4.1^{+1.5}_{-1.2})$ counts/(keV·kg·yr) for the natural detector and $(5.1^{+0.9}_{-0.8})$ counts/(keV·kg·yr) for the enriched BeGe detectors. These values show an improvement in the background suppression with respect to previous experiments of a factor of about one order of magnitude. In particular, this suppression factor for the background applies for the very same detectors from the HdM and IGEX experiments [14-16].

4. – Measurement of the half-life of the $0\nu\beta\beta$ decay of ^{76}Ge with GERDA

The two-neutrino double beta ($2\nu\beta\beta$) decay of atomic nuclei is a second-order process predicted by the SM in which the lepton number is conserved and with an extremely low decay rate. It has been suggested [17, 18] that some constraints on the $0\nu\beta\beta$ nuclear matrix element $\mathcal{M}^{0\nu}$ can be derived from the knowledge of the $2\nu\beta\beta$ nuclear matrix element $\mathcal{M}^{2\nu}$. Also, the value of $\mathcal{M}^{2\nu}$ can be directly compared to the predictions based on charge exchange experiments [19, 20] to verify that the nuclear aspects of the $2\nu\beta\beta$ decay are well described. For these reasons the measurement of the half-life of such decay by the GERDA experiment is of extreme interest.

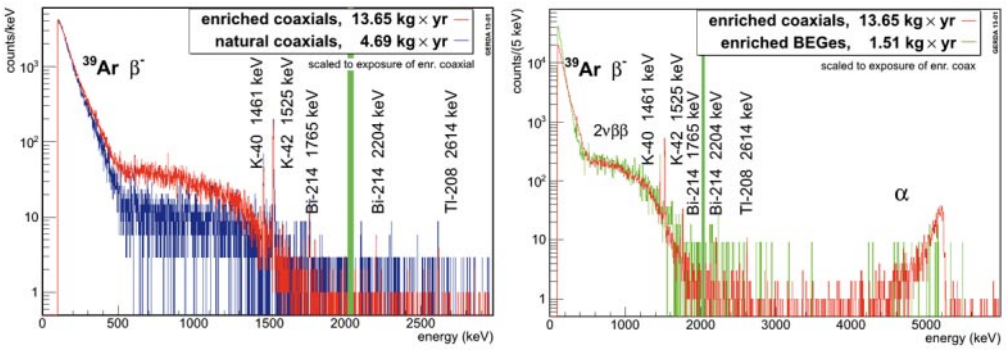

Fig. 3. – Left: Spectra from enriched coaxial detectors (red) and natural detector (blue). Right: Spectra from enriched coaxial detectors (red) and enriched BEGes (green).

The data set for this analysis [21] considers events between 9 November 2011 and 21 March 2012, for a total of 125.9 days and corresponding to an exposure of 5.04 kg yr. The $2\nu\beta\beta$ decay is expected to be the major contributor in the energy spectrum above the endpoint of the ^{39}Ar spectrum, therefore the analysis for the $2\nu\beta\beta$ decay is performed in the range between 600 and 1800 keV, resulting in a total number of events of 8796. The analysis of the resulting energy spectra from the six enriched coaxial diodes is based on a maximum likelihood approach [22]. The experimental energy spectrum is fitted with a globel model. This model contains the $2\nu\beta\beta$ decay of ^{76}Ge and three independent background contributions, ^{42}K, ^{214}Bi and ^{40}K, whose gamma lines are clearly seen from the observed spectra at 1525 keV for ^{42}K, 1460 keV for ^{40}K, 1764 keV for ^{214}Bi. While ^{42}K is a progeny of the ^{42}Ar, ^{214}Bi from the ^{238}U decay series and ^{40}K are gamma emitters from the environmental radioactivity. Other background contributions are not included in the fit since their gamma lines are not clearly seen due to low statistical significance or they are seen only in some detectors. The half-life of the $2\nu\beta\beta$ decay is common in the fit to the six spectra, while the intensities of the background components are considered for each detector independently. Also, the active masses and the ^{76}Ge abundance of each detector are taken as nuisance parameters and integrated at the end of the analysis. For each individual detector the energy spectra for the model components (signal and three background) are obtained from Monte Carlo simulations using the MaGe framework [23] based on Geant4 [24]. The spectral fit is performed using the Bayesian Analysis Toolkit [25]. A flat distribution for the prior probability density function (PDF) for $T^{2\nu}_{1/2}$ is considered between 0 and 10^{22} yr, while the prior PDFs for the active mass fraction and the ^{76}Ge isotopic abundance of each detector are both modeled according to a Gaussian distribution.

In fig. 4 the best fit model, together with experimental data for the sum of the six detectors, is shown. The individual components obtained from the fit are also shown. The best fit model gives an expectation of 8797.0 events divided as: 7030.1 (79.9%) from the $2\nu\beta\beta$ decay of ^{76}Ge; 1244.6 (14.1%) from ^{42}K; 335.5 (3.8%) from ^{214}Bi and 186.8 (2.1%) from ^{40}K. The average signal to background ratio is 4:1 and the model reproduces very well the experimental data, with a p-value of the fit equal to $p = 0.77$.

The resulting best estimate of the half-life is $T^{2\nu}_{1/2} = (1.84^{+0.09}_{-0.08}(\text{stat})^{+0.11}_{-0.06}(\text{syst})) \times 10^{21}$ yr. The systematic uncertainties on $T^{2\nu}_{1/2}$ not included in the fitting procedure include uncertainties related to the fit model, uncertainties due to the Monte Carlo simulation

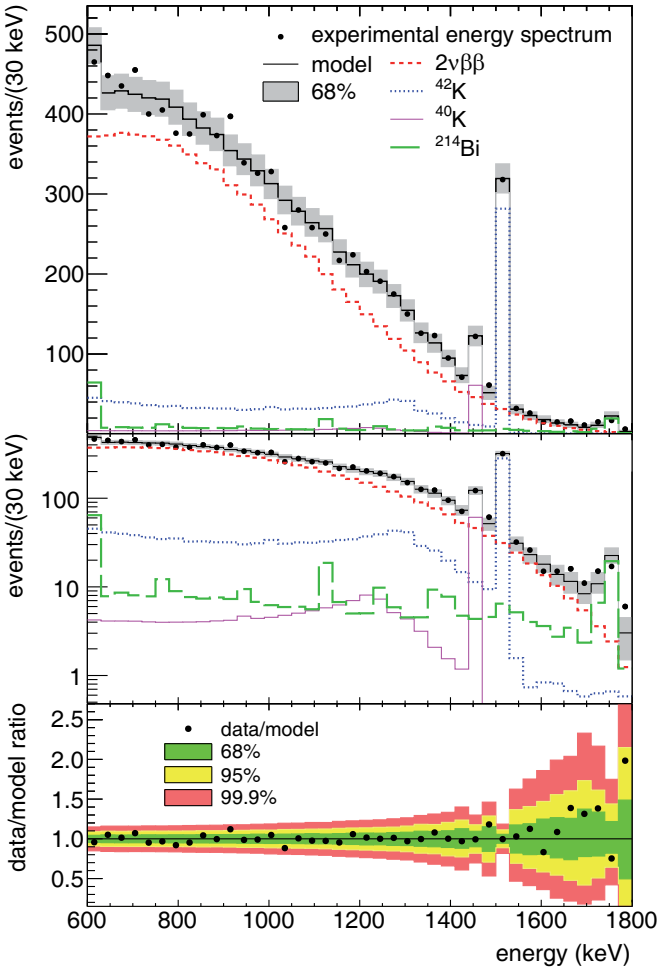

Fig. 4. – Upper and middle panels: Experimental data (markers) and the best fit model (black histogram) for the sum of the six detectors (linear and logarithmic scale). Individual contributions from the decay (red), ^{42}K (blue), ^{40}K (purple) and ^{214}Bi (green) are shown separately. The shaded band indicates the 68% probability range for the data calculated from the expected event counts of the best fit model. Lower panel: ratio between experimental data and the prediction of the best fit model.

details and uncertainties due to the data acquisition and data handling. The combination in quadrature of all these contributions gives a systematic uncertainty of $^{+6.2}_{-3.3}$%, which corresponds to $^{+0.11}_{-0.06} \times 10^{21}$ yr.

The experimental nuclear matrix element for the $2\nu\beta\beta$ decay of ^{76}Ge can be derived from the measured half-life, by using phase space factors from the improved electron wave functions reported in [26]. The result is $\mathcal{M}^{2\nu} = 0.133^{+0.004}_{-0.005}\,\mathrm{MeV}^{-1}$, 11% smaller than that used in [17] and, according to the relation between $\mathcal{M}^{2\nu}$ and $\mathcal{M}^{0\nu}$ described in [17], the new value for $\mathcal{M}^{2\nu}$ corresponds to an increase of about 15% in the predicted half-life for $0\nu\beta\beta$, well within the uncertainty of the model calculation.

5. – Status and outlook

The letter of intent [1] for the GERDA experiment, followed by the Proposal [2] was submitted to LNGS in 2004. The commissioning of GERDA has been completed and phase I data taking started on November, 2011. The exposure reached by the end of 2012 was about 15 kg·yr for the enriched detectors and 5 kg·yr for the natural one, with an average duty cycle of 89%. In the first phase of GERDA the target sensitivity for the half-life of the $0\nu\beta\beta$ decay is about $T^{0\nu}_{1/2} \simeq 2 \cdot 10^{25}$ yr at 90% confidence level, requiring an exposure of about 20 kg·yr. In the second phase about 20 kg of new BEGe ^{76}Ge detectors will be installed. Additionally, the combination of new background suppression techniques like the PMT instrumentation of the liquid argon and the pulse-shape analysis will allow to reach background levels on the order of 10^{-3} counts/(keV·kg·yr) [11].

REFERENCES

[1] The GERDA Collaboration, Letter of Intent (2004).
[2] The GERDA Collaboration, Proposal (2004) http://www.mpi-hd.mpg.de/GERDA.
[3] Klapdor-Kleingrothaus H. V. *et al.*, *Eur. Phys. J. A*, **12** (2001) 147.
[4] Alseth C. E. *et al.*, *Phys. Rev. D*, **65** (2002) 092007.
[5] Klapdor-Kleingrothaus H. V. *et al.*, *Phys. Lett. B*, **586** (2004) 198.
[6] Klapdor-Kleingrothaus H. V. and Krivosheina I. V., *Mod. Phys. Lett. A*, **21** (2006) 1547.
[7] The GERDA Collaboration, *Eur. Phys. J. C*, **73** (2013) 2330.
[8] Heusser G., *Annu. Rev. Nucl. Part. Sci.*, **45** (1995) 543.
[9] Barabanov I. *et al.*, *Nucl. Instrum. Methods A*, **606** (2009) 790.
[10] Zavarise P., PhD Thesis, University of L'Aquila, 2013.
[11] The GERDA Collaboration, Progress Report for the LNGS Scientific Community, Oct. 2012.
[12] Ashitkov V. D. *et al.*, *Instrum. Exper. Techniques*, **46** (2003) 153.
[13] Chkvorets O., PhD Thesis, University of Heidelberg (2008).
[14] The Igex Collaboration, *Phys. Rev. D*, **65** (2002) 092007.
[15] Gonzalez D. *et al.*, *Phys. Rev. C*, **59** (1999) 2108; Gonzalez D. *et al.*, *Nucl. Phys. B Procs.*, **87** (2000) 278; Gonzalez D. *et al.*, *Nucl. Instrum. Methods A*, **515** (2003) 634.
[16] Klapdor-Kleingrothaus H. V. *et al.*, *Nucl. Instrum. Methods A*, **522** (2004) 371.
[17] Rodin V. A., Fässler A., Šimkovic F. and Vogel P., *Nucl. Phys. A*, **766** (2006) 107; Rodin V. A., Fässler A., Šimkovic F. and Vogel P., *Nucl. Phys. A*, **793** (2007) 213(erratum).
[18] Šimkovic F., Hodak R., Fässler A. and Vogel P., *Phys. Rev. C*, **83** (2011) 015502; Caurier E., Nowacki F. and Poves A., *Phys. Lett. B*, **711** (2012) 62; Barea J. and Iachello F., *Phys. Rev. C*, **79** (2009) 044301; Suhonen J. and Civitarese O., *J. Phys. G: Nucl. Part. Phys.*, **39** (2012) 085105.
[19] Grewe E.-W. *et al.*, *Phys. Rev. C*, **78** (2008) 044301.
[20] Ties J. H. *et al.*, *Phys. Rev. C*, **86** (2012) 014304.
[21] The GERDA Collaboration, *J. Phys. G: Nucl. Part. Phys.*, **40** (2013) 035110.
[22] Caldwell A. and Kröninger K., *Phys. Rev. D*, **74** (2006) 092003.
[23] Boswell M. *et al.*, *IEEE Trans. Nucl. Sci.*, **58** (2011) 1212.
[24] The Geant4 Collaboration, *Nucl. Instrum. Methods A*, **506** (2003) 250; The Geant4 Collaboration, *IEEE Trans. Nucl. Sci.*, **53** (2006) 270.
[25] Caldwell A., Kollar D. and Kröninger K., *Comput. Phys. Commun.*, **180** (2009) 2197.
[26] Kotila J. and Iachello F., *Phys. Rev. C*, **85** (2012) 034316.